

Article

# Assessment of Land-Cover/Land-Use Change and Landscape Patterns in the Two National Nature Reserves of Ebinur Lake Watershed, Xinjiang, China

Fei Zhang <sup>1,2,\*</sup>, Hsiang-te Kung <sup>3</sup> and Verner Carl Johnson <sup>4</sup>

<sup>1</sup> College of Resources and Environmental Sciences, Xinjiang University, Urumqi 830046, China

<sup>2</sup> Ministry of Education of Key Laboratory of Oasis Ecology at Xinjiang University, Urumqi 830046, China

<sup>3</sup> Department of Earth Sciences, the University of Memphis, Memphis, TN 38152, USA; hkung@memphis.edu

<sup>4</sup> Department of Physical and Environmental Sciences, Colorado Mesa University, Grand Junction, CO 81501, USA; vjohnson@coloradomesa.edu

\* Correspondence: zhangfei3s@163.com; Tel.: +86-991-8581-281

Academic Editor: Audrey L. Mayer

Received: 16 March 2017; Accepted: 27 April 2017; Published: 2 May 2017

**Abstract:** Land-cover and land-use change (LCLUC) alters landscape patterns and affects regional ecosystems. The objective of this study was to examine LCLUC and landscape patterns in Ebinur Lake Wetland National Nature Reserve (ELWNNR) and Ganjia Lake *Haloxylon* Forest National Nature Reserve (GLHFNNR), two biodiversity-rich national nature reserves in the Ebinur Lake Watershed (ELW), Xinjiang, China. Landsat satellite images from 1972, 1998, 2007 and 2013 were used to calculate the dynamics of a land-cover and land-use (LCLU) transition matrix and landscape pattern index using ENVI 5.1 and FRAGSTATS 3.3. The results showed drastic land use modifications have occurred in ELWNNR during the past four decades. Between 1972 and 1998, 1998 and 2007, and 2007 and 2013, approximately 251.50 km<sup>2</sup> (7.93%), 122.70 km<sup>2</sup> (3.87%), and 195.40 km<sup>2</sup> (6.16%) of wetland were turned into salinized land. In GLHFNNR both low and medium density *Haloxylon* forest area declined while high density *Haloxylon* forest area increased. This contribution presents a method for characterizing LCLUC using one or more cross-tabulation matrices based on Sankey diagrams, demonstrating the depiction of flows of energy or materials through ecosystem network. The ecological landscape index displayed that a unique landscape patches have shrunk in size, scattered, and fragmented. It becomes a more diverse landscape. Human activities like farming were negatively correlated with the landscape diversity of wetlands. Furthermore, evidence of degraded wetlands caused by air temperature and annual precipitation, was also observed. We conclude that national and regional policies related to agriculture and water use have significantly contributed to the extensive changes; the ELWNNR and GLHFNNR are highly susceptible to LCLUC in the surrounding Ebinur Lake Watershed.

**Keywords:** land-cover and land-use change; landscape pattern; landscape index; remote sensing

## 1. Introduction

Land-cover and land-use (LCLU) has been a traditional and important research topic in both local and global environmental studies [1,2]. It is widely acknowledged that LCLUC is a primary cause of the current global biodiversity crisis, mostly through its effects on habitat quality. Numerous studies have reported that LCLUC is the main cause for species extinction worldwide, and also results in species replacement and biotic homogenization or differentiation [3,4]. For example, habitat fragmentation has become one of the main threats to biodiversity at local, regional and global scales and is causing LCLUC [5,6], as well as causing increasing rarity of species and driving many species

toward extinction [3,7,8]. It is well known that human activities and natural processes often accelerate the speed of LCLUC [9,10]. The complex interaction of various social, economic and biophysical situations following agricultural diversification, advancement in technology coupled with alarming rate of population pressure result in LCLUC [11]. Therefore, human factors and natural factors are considered as major driving factors of LCLUC in current study.

Wetlands are the only ecosystems formed as a result of land and water interactions [12]. Wetlands play an important role in many ecosystems by mitigating pollution, providing habitats for plants and wildlife, regulating climate, and preserving biodiversity [13–16].

The Ebinur Lake watershed (ELW), located in Xinjiang Uyghur Autonomous Region, China, is an arid to semi-arid region suffering from frequent droughts and water scarcity and has become the second most significant area of ecological degradation after the Tarim River Basin in Xinjiang. It contains the Ebinur Lake Wetland National Nature Reserve (ELWNNR) and Ganjia Lake *Haloxylon* Forest National Nature Reserve (GLHFNNR). In the last six decades, increased human population density has led to a dramatic expansion of agricultural areas over the ELW, resulting in significant changes in LCLU, i.e., shrinking wetlands. Although wetlands within the ELWNNR and GLHFNNR have been recognized as critical ecosystems and part of oasis ecology, these wetland areas within the ELW are rapidly disappearing, causing the natural wetland habitats and *Haloxylon* forest to shrink because of an increase in human activities in the study area. It is critical to providing essential ecological and environmental services in the study area. The development of the Watershed on the north slope of the economic belt of the Tianshan Mountains region and the Asia-Europe Continental Bridge are very important to the sustainable development of the social economy and oasis ecology in Xinjiang. Therefore, we conducted a comparative examination of LCLUC and landscape patterns in the study area using GIS spatial automatic overlay method and Landsat satellite images collected during 1972, 1998, 2007 and 2013.

Among these available remotely sensed data, the Landsat TM/ETM+ data have been widely used in many case studies of LCLU worldwide, given the free open-access for data acquisition, the long time span, and the spatial coverage for most of the LCLU. Moreover, compared with the coarse resolution TIR data, such as AVHRR and MODIS, the recognition of LULC based on Landsat TM/ETM+ data can produce persuasive results with much greater accuracy [17]. Previous case studies have provided a wealth of useful information, which has allowed us to rethink the adverse consequences of LULC change and rapid urbanization and to therefore help the decision-makers develop and execute rational land use policies. However, studies using a combination of socio-economic analysis and time series Landsat TM/ETM+ data over a long time span were relatively scarce.

The purposes of this study were (i) using remote sensing and geographic information system (GIS) analysis to monitor and analyze the dynamics of LCLUC in the ELWNNR and GLHFNNR, (ii) analyze the changes in landscape patterns using landscape metrics, i.e., number of patches (NP), largest patch index (LPI), landscape shape index (LSI), contagion index (CONTAG), Shannon diversity index (SHDI), Shannon evenness index (SHEI), interspersion and juxtaposition index (IJI), fragmentation index (FI) and aggregation index (AI) and (iii) explore natural and anthropogenic drivers of LCLUC in the study area.

## 2. Materials and Methods

### 2.1. Study Area

Located in the center of Eurasia and in the northwestern part of Xinjiang Uyghur Autonomous Region, the Ebinur Lake watershed lies between 43°38'–45°52' N and 79°53'–85°02' E (Figure 1). Covering a total area of 5062 km<sup>2</sup>, the Ebinur Lake watershed is characterized by mountains, plains and wetland/lake areas. The altitude and slope of Ebinur Lake watershed at the range of 190–5500 m and 3–10‰, respectively. Three major river systems including the Bortala, Jing and Kuitun rivers along with 12 of their tributaries once fed the Ebinur Lake watershed. The Ebinur Lake watershed is mainly

recharged by alpine glacier meltwater and mountain precipitation, totaling  $37.46 \times 10^8 \text{ m}^3/\text{yr}$ . Natural environmental changes and human activities (i.e., modern agricultural development in oases) have caused many rivers to gradually lose their hydraulic connections with Ebinur Lake. Currently, only Bortala and Jing rivers supply water to Ebinur Lake. The typical arid continental climate of the Ebinur Lake watershed features hot summers, chilly winters, rare precipitation events and strong evaporation. The mean annual temperature varies from 4.0 to 8.1 °C, while the mean annual precipitation varies between 102.60 and 229.40 mm from the plain to the mountains, respectively [18].

Figure 1 shows location of the two biodiversity-rich national nature reserves, the Ebinur Lake Wetland National Nature Reserve (ELWNNR) and Ganjia Lake *Haloxylon* forest National Nature Reserve (GLHFNNR). Ebinur Lake Wetland National Nature Reserve is the most representative temperate arid zone wetland ecosystem in China acting as the center of oasis and a region experiencing desertification on the northern slope of the Tianshan Conjugate. It can be characterized as a region of lake-wetlands, marshes and river-wetlands; this wetland area is located in an ecologically fragile district that is one of the few areas of desert species habitat and has critical implications for the environment of the Junggar Basin [19].

The GLHFNNR stands in the western margin of the Gurbantünggüt Desert and adjoins Ebinur Lake. This reserve serves a natural barrier buffering the region against the east wind that blows into the Ebinur Lake region. The GLHFNNR has the largest of area and preserve of intact white *Haloxylon* forest. The *Haloxylon* forest generally grows in the Gobi desert, salt desert and migratory dunes. *Haloxylon* forest also serves in sand stabilization, regulating climate, maintaining biodiversity and protecting landscape resources. This reserve is not only part of China's "Three North" forest protection system (a forest restoration program started in 1978, designed to be completed in 2050), but also resists to the raging winds from Ala Mountain and controls mobile sand dunes. Therefore the GLHFNNR is the one of the most important areas for protecting the natural environment of this arid area [20]. In recent years, with the reduction of *Haloxylon* forest area, the influence of changes in local rainfall and lower humidities have affected the changes in the patterns of the *Haloxylon* forest ecosystem and landscape [21].

Because of high evapotranspiration and low rainfall, regions where evaporation occurs on the edges or shallow areas of the Ebinur Lake area are prone to salinization. In addition, salinity often leads to other major soil degradation processes such as soil compaction and dispersion, as well as increased corrosion from the saline soil around man-made structures [22]. Therefore, soil salinization in Ebinur Lake can and will threaten the natural environment and related resources such as human land use of these areas and may limit our ability to maintain sustainable development [23]. Figure 2 provides photos of the physical appearances of the ELWNNR and GLHFNNR landscape.

## 2.2. Image Processing

Four Landsat images were used in this study as follows: Multi-spectral Scanner images collected on 25 September 1972; Thematic Mapper images from 2 September 1998 and 11 September 2007; Operational Land Imager images from 2 September 2013. All the information about the data sources is shown in Table 1. All of these images were downloaded from the United States Geological Survey website (<http://glovis.usgs.gov/>) for LCLU classification in this study. Images have a minimal cloud cover of 2–3%; these satellite images were originally rectified to Universal Transverse Mercator projection. The images were acquired on different dates with slightly different seasons, the images were geometrically rectified to the local coordinate system of Ebinur Lake watershed using 50 ground control points symmetrically distributed across the images. A nearest neighbor method was used for resampling when conducting rectification, with an error of less than one pixel. Finally, the resolution of all images is resampled to 30 m, so it was crucial to make a radiance calibration and atmospheric correction to all images, using the FLAASH tools provided by ENVI 5.1 (ENVI, Version 5.1, Exelis Visual Information Solutions, Boulder, CO, USA, 2013) to convert the radiance to reflectance [12,24].

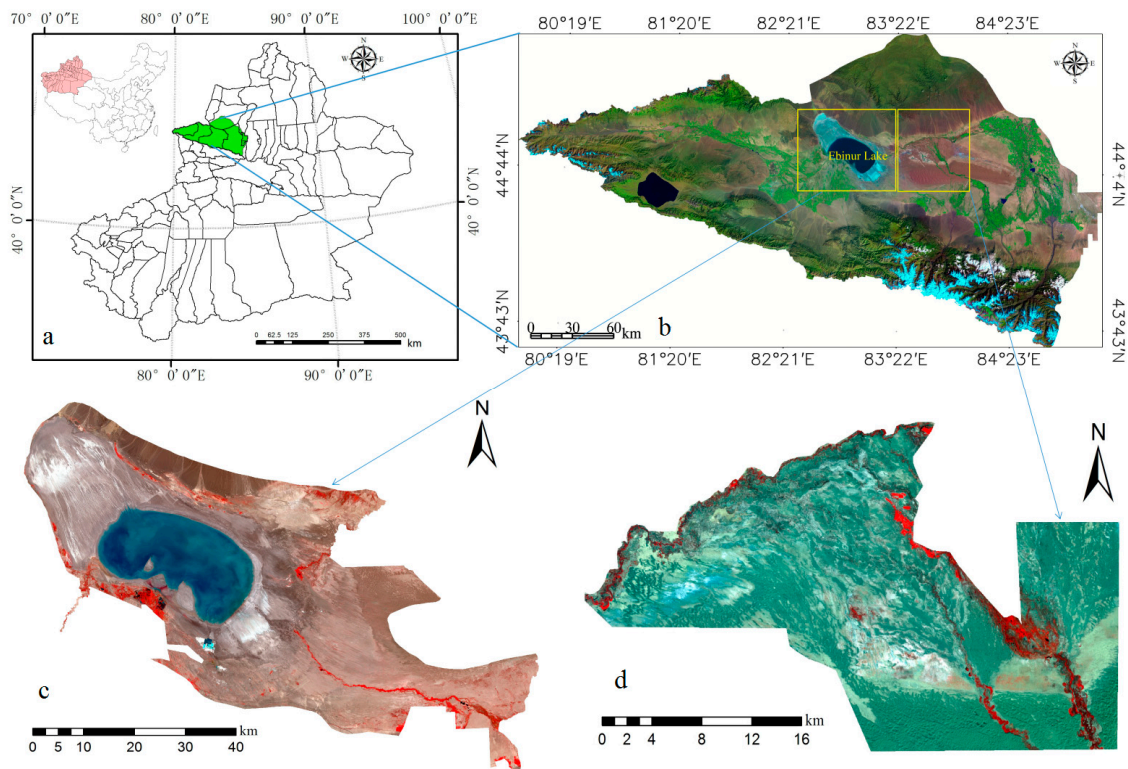


**Figure 1.** Location maps of the study area: (a) vicinity map showing the location of the study area within Xinjiang and China; (b) map of the Ebinur Lake vicinity; (c) Ebinur Lake Wetland Nature Reserve; (d) Ganjia Lake *Haloxylon* Forest Nature Reserve.

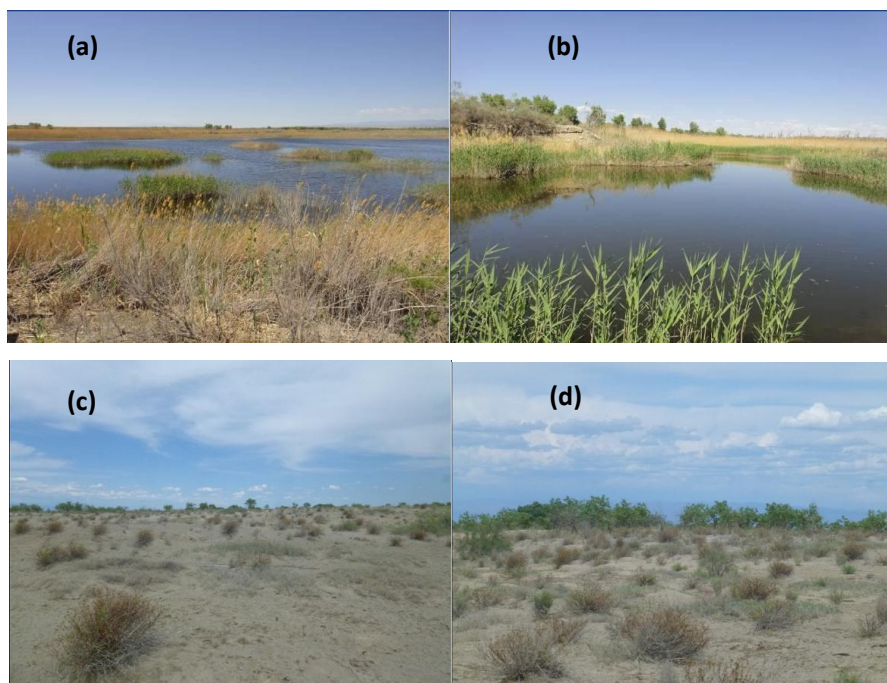


**Figure 2.** Landscape photos of study area (Photographed by Fei Zhang): (a,b) are Ebinur Lake Wetland National Nature Reserve; (c,d) are Ganjia Lake *Haloxylon* Forest National Nature Reserve; (a,b) show Ebinur Lake marshes with sparse vegetation. (c,d) show the desert appearance with *Haloxylon* forest.

**Table 1.** Data sources of landscape information in ELWNNR and GLHFNNR.

Number	Imaging Data	Sensor	Resolution (m)	Spectral Bands
1	21 September 1972	MSS	80	B1, B2, B3, B4
2	25 September 1998	TM	30	B1, B2, B3, B4, B5, B7
3	18 September 2007	TM	30	B1, B2, B3, B4, B5, B7
4	26 August 2013	OLI_TIRS	30	B1, B2, B3, B4, B5, B6, B7

### 2.3. Methods

#### 2.3.1. LCLU Classification Methods

Researchers have proposed and experimented with many LCLU classification methods in recent years [25–27]. In comparison with various novel classifiers, the traditional maximum likelihood classifier has generally been used because of its ease in application, simple operation and good performance [28]. In this study, a supervised classification based on the maximum likelihood classification (MLC) method was employed to classify the individual images independently. MLC is the most common type of supervised classification and has been widely used in the literature [24,29–32]. This method has considered not only the mean or average values in assigning classification, but also the variability of brightness values in each class [33]. Therefore, in this paper, the landscape of the ELWNNR was classified using six LCLU types. Land use types included water body and forestland. Land cover types included salinized land, desert, wetland and other objects including medium-, low-cover grasslands, and bare land. The GLHFNNR was classified using four land cover types, i.e., high (HDHF), medium (MDHF), and low (LDHF) density *Haloxylon* forest as well as desert.

We optimized the classification accuracy and adjusted it by field sampling using GPS device (G350, UniStrong, Beijing, China, 2014). Both computer classification obtained by using ENVI 5.1 software and manual interpretation were used to obtain the land use information [1]. Then, we collected 100 random samples as training data and combined this data with field data that were used in the maximum likelihood classifier to do the classification. Based on the land-use classification system of the China Agricultural Planning Committee (1984) and the actual situation of ELWNNR, six land use/cover categories were delineated: water body (including lakes, rivers, ponds, and reservoirs), vegetation (trees, grass, bushes, sparse trees, shrubs, and other vegetation), salinized land, desert, wetland (including salt marshes, beaches, flood plains, swamps, and bogs) and others objects (including medium-, and low-cover grasslands, and bare land). For this paper we selected more than 600 pixels of each land use/cover type as areas of interest.

#### 2.3.2. Accuracy Assessment

The accuracy of the different thematic maps produced from the classifiers; accuracy assessment was performed based on the computation of the error matrix statistics. As a result, the overall accuracy (OA), user's accuracy (UA), producer's accuracy (PA) and the kappa coefficient (Kc) were computed [34]. The classification accuracy was verified according to the Kappa coefficient that is a statistic which measures inter-rater agreement for qualitative items [35]. Fleiss's [36] equally arbitrary guidelines characterize kappa coefficient over 0.75 as excellent, 0.40 to 0.75 as fair to good, and below 0.40 as poor.

### 2.3.3. Land-Cover and Land-Use Transition Matrix

A land-cover and land-use transition matrix was generated to reflect the changes of land-cover and land-use types in two stages. We used the following equation to calculate the matrix [37]:

$$p = \begin{bmatrix} p_{11} & p_{12} & \cdots & p_{1j} \\ p_{21} & p_{22} & \cdots & p_{2j} \\ \vdots & \vdots & \vdots & \vdots \\ p_{i1} & p_{i2} & \cdots & p_{ij} \end{bmatrix}$$

where  $p_{ij}$  indicates the area in transition from landscape  $i$  to  $j$ . Each element of the transition matrix is (1)  $p_{ij}$  is non-negative and (2)  $\sum_{j=1}^n p_{ij} = 1$ .

Sankey diagrams are often used to analyze energy or material flows, with arrows representing flows and the thickness of the arrow representing the magnitude of the flow [38]. For two categorical LCLU maps that used the same set of  $N$  categories, there are  $N \times (N - 1)$  potential forms of map differences, consisting of pixels classified as category  $i$  in one map and category  $j$  in the other map. There are  $N$  instances of map differences or similarity, or groups of pixels that are classified as the same category in both maps. Map differences and similarity are associated with land use changes, i.e., differences for a change and similarity for no change, respectively. These change status in the transition matrix can be represented in the Sankey diagram by a persistence or transition line [39].

Sankey diagram were used on visualization of LCLUC dynamics in the ELWNNR and GLHFNNR. This diagram provided the classification results from four maps, and the LCLU dynamics observed in three time intervals: 1972–1998, 1998–2007 and 2007–2013. A transition matrix, which compares the two maps within each time interval, is also presented.

### 2.3.4. Landscape Index

A landscape pattern index is an indicator of spatial landscape patterns, which reflects the characteristics of the landscape composition and spatial configuration. Quantification is one of the essential goals of landscape ecology [1,40]. Because landscape metrics are highly correlated [41,42], the correlated metrics were deselected to reduce redundancy, then nine landscape indices were chosen to display the land cover/land use changes in the study area. These indices include number of patches (NP), largest patch index (LPI), landscape shape index (LSI), contagion index (CONTAG), Shannon diversity index (SHDI), Shannon evenness index (SHEI), interspersion and juxtaposition index (IJI), fragmentation index (FI) and aggregation index (AI). The landscape parameters for each LCLU type was calculated for 1972, 1998, 2007 and 2013 using the FRAGSTATS 3.3 software [13]. Landscape indices in FRAGSTATS 3.3 are quite effective for describing landscape changes and refer to both human activities and natural effects [2,17,43] (Table 2).

**Table 2.** Landscape metrics used in the present study.

Index	Symbol	Definition	Formula
Number of Patches	NP	Number of patches divided by area.	$NP = N_i$
Largest Patch Index	LPI	LPI quantifies the percentage of total landscape area comprised by the largest patch. As such, it is a simple measure of dominance.	$LPI = \frac{Max(a_1, \dots, a_n)}{A} (100)$

Table 2. Cont.

Index	Symbol	Definition	Formula
Landscape Shape Index	LSI	A perimeter-to-area ratio that measures the overall geometric complexity of the landscape. LSI provides a standardized measure of total edge or edge density that adjusts for the size of the landscape.	$LSI = \frac{25 \sum_{k=1}^m e_{ik}}{\sqrt{A}}$
Contagion Index	CONTAG	Measures the extent to which patch types are aggregated or clumped. CONTAG is inversely related to edge density.	$CONTAG = \left[ 1 + \sum_{i=1}^m \sum_{j=1}^n \frac{P_{ij} \ln(P_{ij})}{2 \ln(m)} \right] (100)$
Shannon's Diversity Index	SHDI	SHDI is a popular measure of diversity in community ecology, applied here to landscape. SHDI is somewhat more sensitive to rare patch types than Simpson's diversity index.	$SHDI = - \sum_{i=1}^m (P_i \cdot \ln P_i)$
Shannon's Evenness Index	SHEI	SHEI is expressed such that an even distribution of area among patch types results in maximum evenness.	$SHEI = \frac{\sum_{i=1}^m (P_i \cdot \ln P_i)}{\ln m}$
Interspersion and Juxtaposition Index	IJI	IJI is based on patch adjacencies, not cell adjacencies like the contagion index.	$IJI = \frac{- \sum_{k=1}^m \left[ \left( \frac{e_{ik}}{\sum_{k=1}^m e_{ik}} \right) \ln \left( \frac{e_{ik}}{\sum_{k=1}^m e_{ik}} \right) \right]}{\ln(m-1)} (100)$
Fragmentation Index	FI	FI is appealing because it reflects shape complexity across a range of spatial scales (patch sizes).	$FI = \frac{N_i}{CA_i}$
Aggregation	AI	AI takes into account only the like adjacencies involving the focal class, not adjacencies with other patch types.	$AI = 2 \ln(m) + \sum_{i=1}^m \sum_{j=1}^n P_{ij} \ln(P_{ij})$

Note:  $i = 1, \dots, m$  patch types (classes);  $j = 1, \dots, n$  patches;  $k = 1, \dots, m$  patch types (classes);  $A =$  total landscape area ( $m^2$ );  $a_{ij} =$  area ( $m^2$ ) of patch  $ij$ ;  $P_{ij} =$  perimeter (m) of patch  $ij$ .  $e_{ik} =$  total length (m) of edge in landscape between patch types (classes)  $i$  and  $k$ , includes landscape boundary;  $N =$  total number of patches in the landscape, excluding any background patches;  $N_i =$  number of patches in the landscape of patch type (class)  $i$ ;  $m =$  number of patch types (classes) present in the landscape, excluding the landscape border if present;  $P_i =$  proportion of the landscape occupied by patch type (class)  $i$ .

### 2.3.5. Driving Factor Analysis

LCLUC is a central factor related to changes in the Earth's climate, the environment in a broad sense and human society. Policymakers seek for scientific information about the forces driving LCLUC so that they may not only focus on symptoms, but on the causes of LCLUC [44]. The analysis on driving forces of LCLUC is one of the vital parts of LCLUC research. The relationship between LCLUC and driving forces of LCLUC is often quantified by combining a use conceptual model with a mathematical model, introducing mathematical/statistical methods and adopting both historical and current LCLUC data. The driving factors of LCLUC include natural processes and human interventions, such as topography, climate change, human activity and government policies. It is crucial for us to evaluate the predominant factors in LCLUC to allow policy makers to deal with this change. The authors chose representative driving forces (natural, human and policy driving factors) to explore the relationships between driving factors and LCLUC [44]. Figure 3 shows a technical flowchart of this research study.

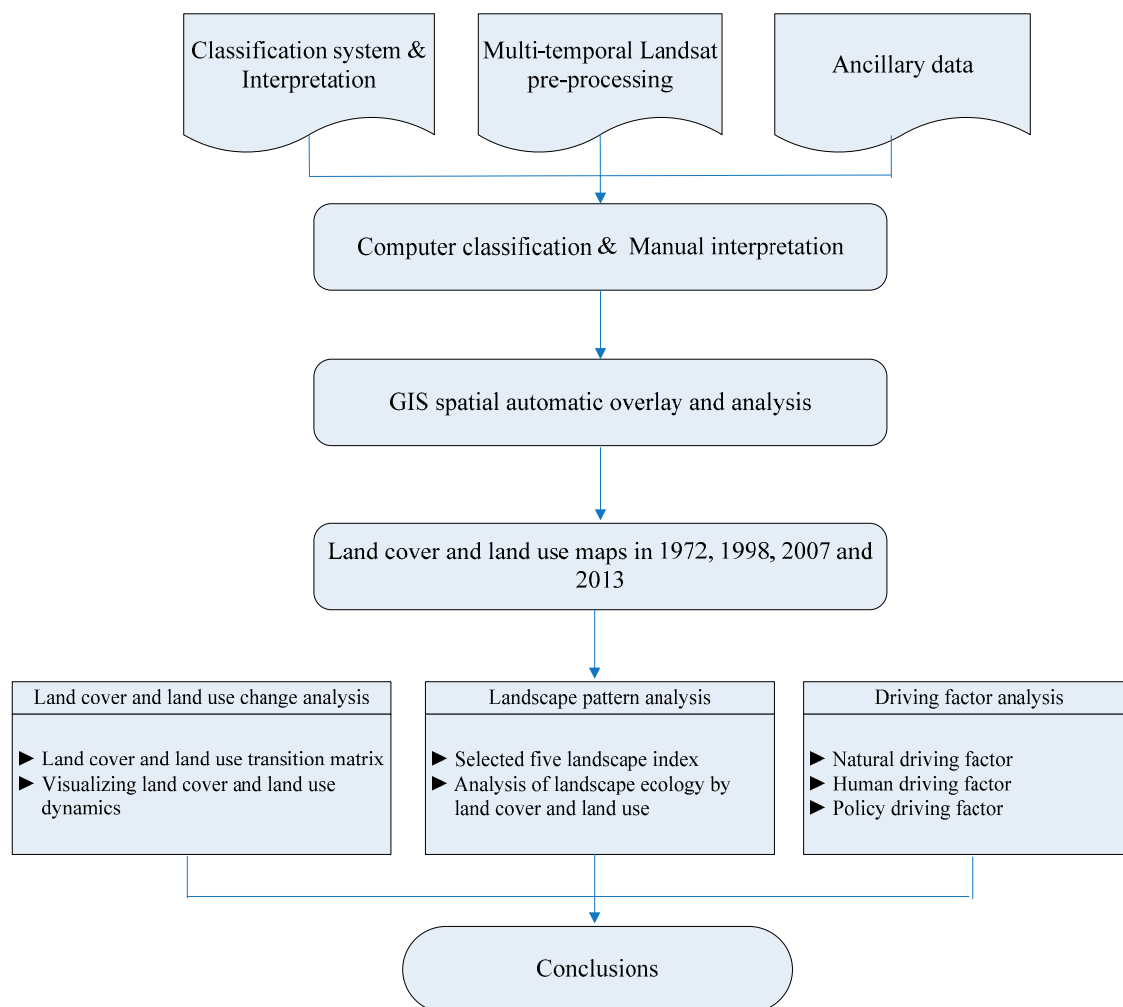


**Figure 3.** Flowchart for the land-cover and land-use change and landscape pattern changes in the study area.

### 3. Results and Analyses

#### 3.1. Land-Cover and Land-Use Changes in the ELWNNR

The four classified images in (Figure 4) were used to calculate each landscape index. Table 3 shows the summary of LCLUC in the ELWNNR in the last 21 years. Land use policies are regulated by the national and regional government agencies. The Chinese government promotes “cottons as the key to the economy”, in this area and encouraged the development of western China, including Ebinur Lake Watershed for intensive cotton farming, and these policies result in that salinized land increased to the greatest extent, with an annual average growth rate of 4.83%. Wetland area also decreased and water area shrunk significantly. Forestland areas increased during the study period, although the area covered by trees near the river decreased and the area covered by shrubs far from water increased. Forestland was preferred for agricultural reclamation, thus forestland areas decreased during the study period because of excessive land reclamation, and the change leads to succession of LCLU structure [45]. Table 4 shows the confusion matrix to verify the classification results between 1972, 1998, 2007 and 2013 in the ELWNNR in the last 21 years.

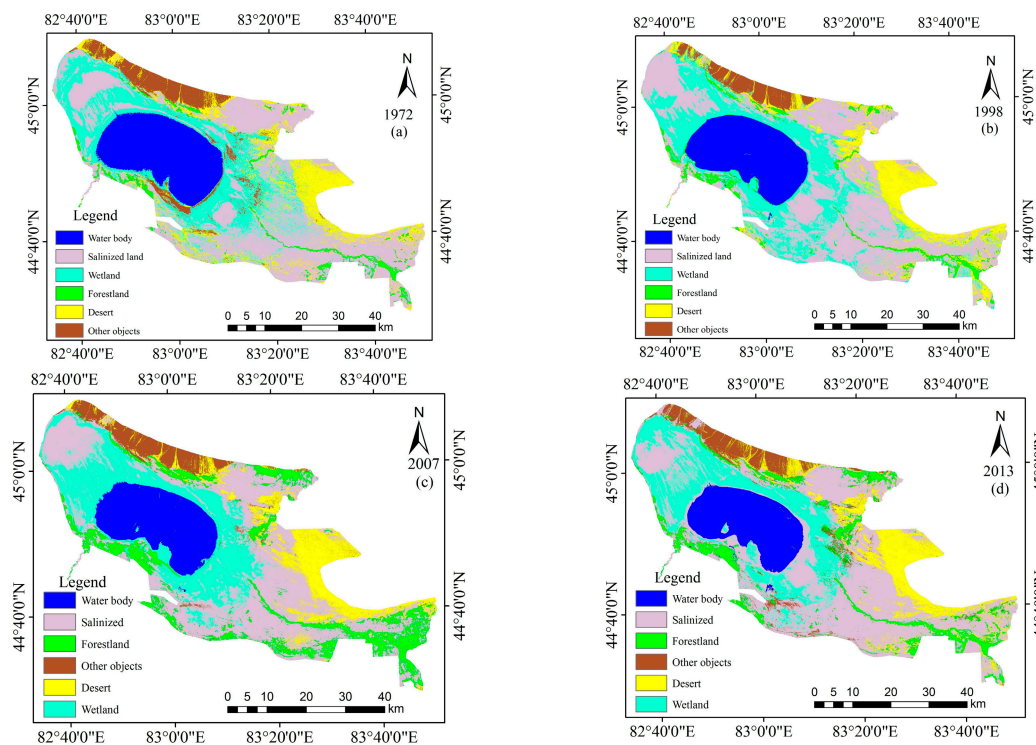


**Figure 4.** The land cover/land use classification maps in ELWNNR in 1972 (a); 1998 (b); 2007 (c) and 2013 (d).

**Table 3.** Changes in land use/cover types in the ELWNNR as measured in 1972, 1998, 2007 and 2013.

Land Cover/Use Types	1972		1998		2007		2013	
	Area (km <sup>2</sup> )	Area Ratio (%)	Area (km <sup>2</sup> )	Area Ratio (%)	Area (km <sup>2</sup> )	Area Ratio (%)	Area (km <sup>2</sup> )	Area Ratio (%)
Water body	538.44	16.98	506.66	15.98	437.56	13.80	406.77	12.83
Salinized land	1203.62	37.96	1243.42	39.21	1180.31	37.22	1371.44	43.25
Forestland	90.67	2.86	114.16	3.60	373.45	11.78	249.46	7.87
Other objects	229.76	7.25	128.52	4.05	171.73	5.42	200.74	6.33
Desert	354.47	11.18	380.53	12.00	351.22	11.08	354.06	11.17
Wetland	754.58	23.80	798.13	25.17	657.22	20.73	588.73	18.57

**Table 4.** Calculation of confusion matrix by Maximum likelihood supervised classification in ELWNNR.

	Water Body	Salinized Land	ForestLand	Desert	Wetland	Other Objects	Total	User's Accuracy (%)
1972	Water body	144	0	0	0	0	144	100
	Salinized land	0	57	0	0	19	102	55.88
	Forestland	0	46	101	0	0	147	68.71
	Desert	4	0	0	114	0	118	96.61
	Wetland	0	0	0	0	99	116	85.34
	Other objects	0	0	0	0	0	77	100
	Total	118	103	101	114	118	120	Overall accuracy = 83.38%
Producer's accuracy (%)	99.61	55.34	100	100	91.67	64.17	Kappa = 0.80	
1998	Water body	99	0	0	0	0	99	100
	Salinized land	0	121	0	0	7	128	94.53
	Forestland	0	0	0	131	0	131	100
	Desert	0	0	0	0	105	105	100
	Wetland	17	0	71	0	0	88	80.68
	Other objects	0	0	49	0	0	128	73.32
	Total	116	121	120	131	112	128	Overall accuracy = 89.97%
Producer's accuracy (%)	85.34	100	59.17	100	93.75	100	Kappa = 0.88	

Table 4. Cont.

	Water Body	Salinized Land	ForestLand	Desert	Wetland	Other Objects	Total	User's Accuracy (%)
2007	Water body	99	0	0	0	0	99	100
	Salinized land	0	114	31	0	7	152	75
	Forestland	17	0	0	120	0	137	87.59
	Desert	0	0	0	0	104	105	99.05
	Wetland	0	7	89	11	1	108	82.41
	Other objects	0	0	0	0	0	127	100
	Total	116	121	120	131	112	128	Overall accuracy = 89.7%
	Producer's accuracy (%)	85.34	94.21	74.17	91.6	92.86	99.22	Kappa = 0.88
2013	Water body	111	0	0	0	0	111	100
	Salinized land	0	76	0	0	15	112	67.86
	Forestland	0	0	0	114	0	135	74.81
	Desert	0	0	0	0	99	116	85.34
	Wetland	7	27	101	0	0	135	74.81
	Other objects	0	0	0	0	4	82	95.35
	Total	118	103	101	114	118	120	Overall accuracy = 86.5%
	Producer's accuracy (%)	94.07	73.79	100	100	83.9	68.33	Kappa = 0.84

### 3.2. Land-Cover Transition Matrix in the ELWNNR

Land-cover maps from 1972, 1998, 2007 and 2013 were analyzed to generate the land cover transition matrices (Table 5). Between 1972 and 1998, 1998 and 2007, and 2007 and 2013, approximately 251.50 km<sup>2</sup> (7.93%), 122.70 km<sup>2</sup> (3.87%), and 195.40 km<sup>2</sup> (6.16%) of wetland were turned into salinized land, respectively. During the 21-year study period, most of the changes of LCLU in ELWNNR were due to anthropogenic factors (i.e., human disturbance) and natural forcing such as ecological succession [19]. The population rate is continuously high and this led to the human disturbance to ELWNNR that caused the increase of farmland. Rising temperatures led to the high evaporation and the balance between evaporation and precipitation is being disturbed and led to the ecological succession in ELWNNR [21].

**Table 5.** Land-cover and land-use change transition matrix from 1972 to 1998, 1998 to 2007 and 2007–2013 (unit: % change).

Periods		Salinized Land	Wetland	Water Body	Desert	Forestland	Other Objects
1972–1998	Salinized land	25.41	10.61	0.03	2.54	0.27	0.33
	Wetland	7.93	12.17	0.77	1.81	0.24	2.28
	Water body	0.00	0.05	15.92	0.00	0.00	0.00
	Desert	3.64	0.63	0.00	6.44	0.58	0.70
	Forestland	0.93	0.33	0.27	0.20	1.81	0.05
	Other objects	0.00	0.01	0.00	0.16	0.01	3.87
1998–2007	Salinized land	27.03	9.02	0.13	0.88	0.15	0.00
	Wetland	6.16	12.31	1.94	0.00	0.30	0.00
	Water body	0.00	0.01	13.78	0.00	0.01	0.00
	Desert	2.31	1.13	0.00	7.43	0.00	0.21
	Forestland	3.62	1.87	0.13	3.04	3.12	0.00
	Other objects	0.09	0.82	0.00	0.65	0.02	3.84
2007–2013	Salinized land	30.56	5.68	0.93	2.44	3.50	0.13
	Wetland	3.87	14.40	0.16	0.00	0.13	0.01
	Water body	0.01	0.09	12.72	0.00	0.01	0.00
	Desert	1.05	0.00	0.00	8.17	1.24	0.71
	Forestland	0.76	0.34	0.00	0.14	6.51	0.11
	Other objects	0.96	0.21	0.00	0.31	0.40	4.45

Figure 5 shows a Sankey diagram of extent of LCLUC in the ELWNNR and change occurring from 1972 to 1998, 1998 to 2007 and 2007 to 2013. The MDHF and LDHF NP values showed the tendency of growth as time goes by, indicating fragmentation of MDHF and LDHF caused by human

disturbance like agricultural reclamation, high population. The agricultural reclamation changed the fragment of HDHF, decreased the HDHF into MDHF as well as LDHF. The stacked bars show the relative abundance of each LCLU type in 1972, 1998, 2007 and 2013. The height of each component is proportional to the relative abundance of the represented land cover, and classified types are arranged vertically from the largest to the smallest. Table 5 provides three transition matrices showing the extent of LCLUC for each LCLU type as well as the size and change trajectories of LCLUC during the three time intervals analyzed here. Four stacked vertical bars in Figure 5 represents land cover of a specific year, and three sets of transition lines positioned between each pair of stacked bars.

The salinized land type is predominant in all four years (Figure 5), comprising 37.90%, 39.20%, 37.20% and 43.20% of the total area in 1972, 1998, 2007, and 2013, respectively. The wetland and the small-extent forestland areas, water body, desert and other objects types all remained relatively stable throughout the study period. At last, the spatial extent of the water body decreased throughout the examined time periods of 1972–1998, 1998–2007 and 2007–2013.

The four stacked bars have the same horizontal width with varying lengths of lines proportional to the length of the time interval. A slightly darker shade of color in Figure 5 express transition lines for each category. To reduce visual confusion, the threshold value was set to 0.30% of the total map area when making this stacked bar to exclude smaller changes.

From 1972 to 2013, the extent of water bodies declined (Figure 5). The increase in the spatial extent of the salinized land occurring from 1972 to 1998 and from 2007 to 2013 are attributed to the conversion of wetlands (Table 5: 10.61% of map from 1972 to 1998, 9.02% from 1998 to 2007 and 5.68% from 2007 to 2013), and to a lesser extent desert (2.54% of map from 1972 to 1998, 0.88% from 1998 to 2007 and 2.44% from 2007 to 2013).

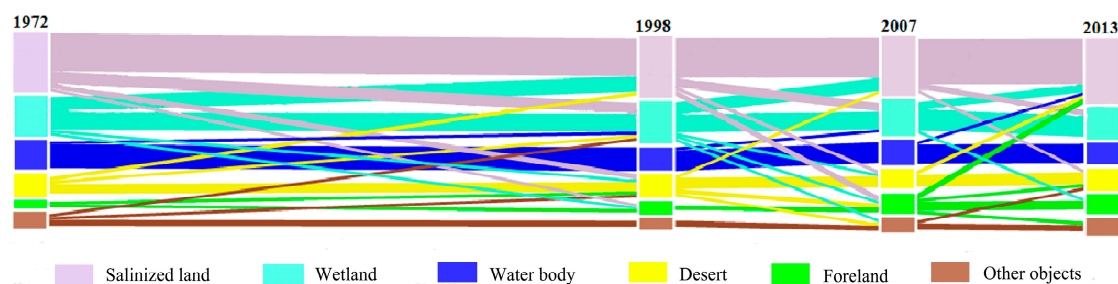


**Figure 5.** Sankey diagram for comparison of land-cover and land-use dynamics in three time intervals defined by four land cover/use maps from the years 1972, 1998, 2007 and 2013 in the Ebinur Lake National Nature Reserve.

### 3.3. Landscape Pattern Analysis—ELWNNR

The NP of desert peaked in 2013 (Figure 6a), indicating that desert patches were small, highly heterogeneous, and fragmented. The NP of wetland was second highest, indicating that agricultural development and reclamation have decreased the size of wetlands and fragmented wetlands. The NP of water body was the lowest that showed slight disturbance. Largest patch index (LPI) demonstrated three development stages (Figure 6b). The LPI of salinized land was the highest as the dominant LCLU type in the ELWNNR. The increasing trend in LPI suggested that the degree of fragmentation and human disturbance are low in the study area. Landscape shape index (LSI) is an effective measure for cluster landscapes. There are also a rising trend of the LSI of water and forest land, showed a more complex patch shape by contrast to other landscape types (Figure 6c). Salinized land displayed high LSI than other landscape types, showed irregular shapes of the region. On the contrary, the LSI of water body are the lowest and indicated that there were fewer changes of water as the time goes by. Different types of ecological landscapes have quite different degrees of aggregation (Figure 6d), indicating that the variety of landscapes with varying degrees of patch connection is different. The CONTAG and SHDI showed an inconsistent trend in the ELWNNR (Figure 6e,f). The CONTAG showed less

fragmentation and enhanced connectivity in the landscape. The negative trend of SHDI indicated a decrease in the wetland landscape types. The SHEI was applied to describe the even distribution of area among patch types, which results in maximum evenness, such as evenness as the complement of dominance (Figure 6g). Therefore, the spatial continuity of landscape patches had also changed and transformed significantly. The IJI exhibited an increasing trend (Figure 6h) indicating that patches became more inter-conjugated and better connected in large scale patches, leaving only a few dominant and leading LCLU types. The FI demonstrated a decrease from 0.06 in 1972 to 0.04 in 2013 (Figure 6i). Severe fragmentation would influence the development of agriculture and pasture livestock. So, the ELWNNR shifted toward a mono-culture land status that hard to preserve its biodiversity, and assumedly resulting from increased human activities and related disturbances for domestic, industrial, and agricultural purposes [46].

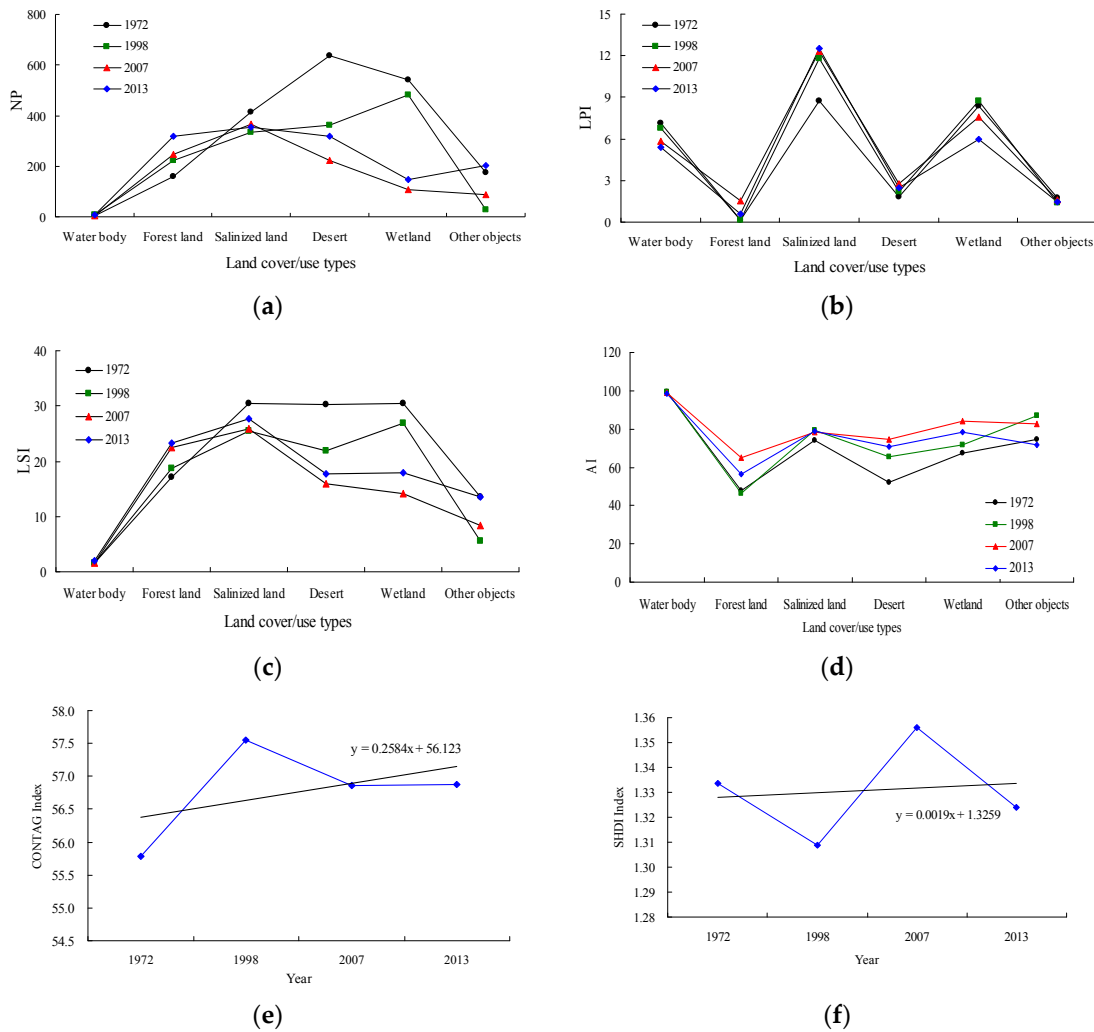
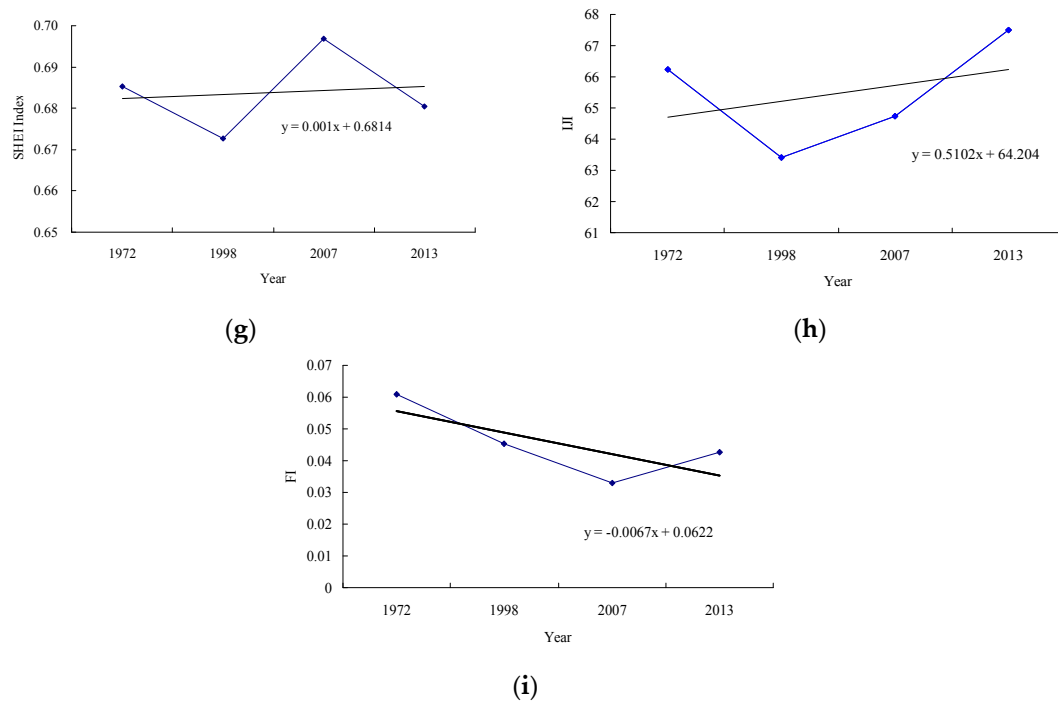


Figure 6. Cont.



**Figure 6.** Comparison of (a) NP, number of patches; (b) LPI, largest patch index; (c) LSI, landscape shape index; (d) AI, aggregation index; (e) CONTAG, contagion index; (f) SHDI, Shannon diversity index; (g) SHEI, Shannon evenness index; (h) IJI, interspersion and juxtaposition index; and (i) FI, fragmentation index values, in the Ebinur Lake Wetland National Nature Reserve at five points in time: 1972, 1998, 2007 and 2013.

### 3.4. Land-Cover and Land-Use Changes in the GLHFNNR

LCLUC were estimated according to the classification results in the GLHFNNR (Figure 7) from satellite images captured in 1972, 1998, 2007 and 2013. Table 6 shows that the main LCLU types in the GLHFNNR are LDHF and MDHF. LDHF area decreased by 19.02 km<sup>2</sup>, MDHF area decreased by 3.36 km<sup>2</sup>, and HDHF area increased by 26.59 km<sup>2</sup> between 1972 and 2013. This indicated that the areas of LDHF lost were result from both human and natural factors like the increase in human disturbance, increased temperature, etc. [46,47]. As described the driving factors before, human factors like high population and excessive agricultural reclamation have changed the structure of GLHFNNR. The increased temperatures led to high evaporation, and disturbed the balance between evaporation and precipitation [21,46]. Table 7 shows the confusion matrix to verify the classification results between 1972, 1998, 2007 and 2013 in the GLHFNNR in the last 21 years.

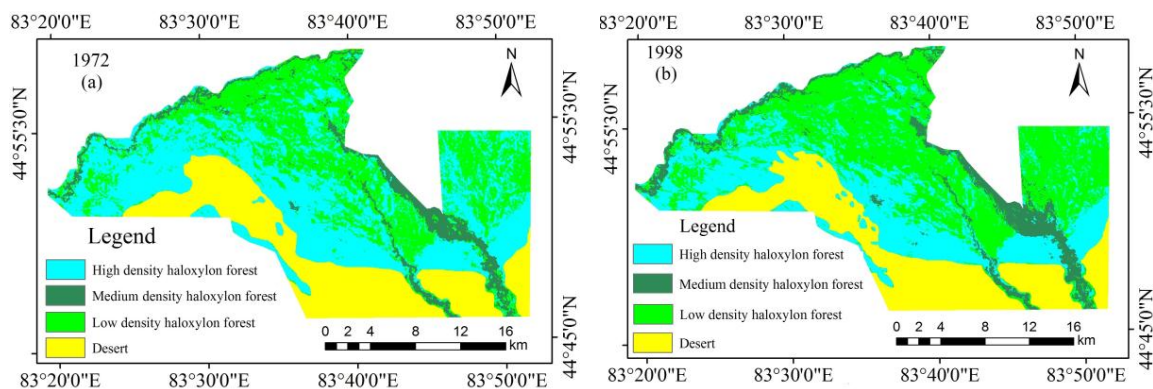


**Figure 7.** Cont.

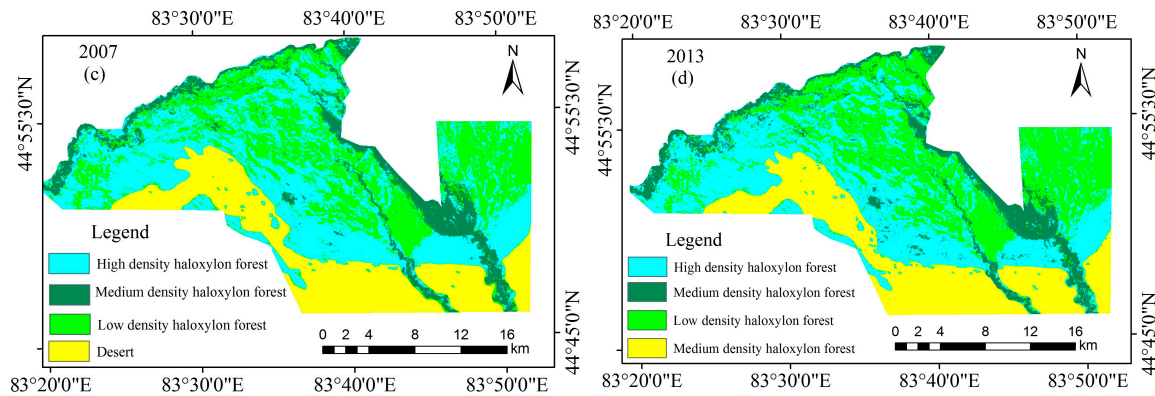


**Figure 7.** Land-cover and land-use classification maps in Ganjia Lake *Haloxylon* Forest National Nature Reserve at five points in 1972 (a); 1998 (b); 2007 (c) and 2013 (d).

**Table 6.** Land-cover and land-use changes in the Ganjia Lake *Haloxylon* Forest National Nature Reserve as measured in 1972, 1998, 2007 and 2013.

Land Cover Types	Area in 1972 (km <sup>2</sup> )	Area Ratio in 1972 (%)	Area in 1998 (km <sup>2</sup> )	Area Ratio in 1998 (%)	Area in 2007 (km <sup>2</sup> )	Area Ratio in 2007 (%)	Area in 2013 (km <sup>2</sup> )	Area Ratio in 2013 (%)
LDHF	228.32	40.42	169.65	30.04	226.43	40.09	209.30	37.06
MDHF	166.52	29.48	215.32	38.12	150.68	26.68	163.15	28.89
HDHF	38.11	6.75	49.87	8.83	61.49	10.89	64.70	11.46
Desert	131.86	23.35	129.97	23.01	126.21	22.35	127.66	22.60

**Table 7.** Calculation of confusion matrix by Maximum likelihood supervised classification in GLHFNNR.

	High Density <i>Haloxylon</i> Forest	Medium Density <i>Haloxylon</i> Forest	Low Density <i>Haloxylon</i> Forest	Desert	Total	User's Accuracy (%)
1972	High density <i>haloxylon</i> forest	33	3	0	36	91
	Medium density <i>haloxylon</i> forest	0	33	3	36	91
	Low density <i>haloxylon</i> forest	0	8	84	92	91
	Desert	0	0	0	94	100
	Total	33	44	87	94	Overall accuracy = 93.25
	Producer's accuracy (%)	100	75	96	100	Kappa = 0.89
1998	High density <i>haloxylon</i> forest	43	3	0	46	93
	Medium density <i>haloxylon</i> forest	0	34	2	36	94
	Low density <i>haloxylon</i> forest	0	6	86	92	93
	Desert	0	0	0	94	100
	Total	43	43	88	94	Overall accuracy = 95
	Producer's accuracy (%)	100	79	97	100	Kappa = 0.90
2007	High density <i>haloxylon</i> forest	36	3	0	39	92
	Medium density <i>haloxylon</i> forest	0	33	3	36	91
	Low density <i>haloxylon</i> forest	0	8	84	92	100
	Desert	0	0	0	94	100
	Total	36	44	87	94	Overall accuracy = 95.75
	Producer's accuracy (%)	100	75	96	100	Kappa = 0.91
2013	High density <i>haloxylon</i> forest	39	3	0	42	92
	Medium density <i>haloxylon</i> forest	0	33	3	36	91
	Low density <i>haloxylon</i> forest	0	12	80	92	86
	Desert	0	0	0	94	100
	Total	39	48	87	94	Overall accuracy = 92.25
	Producer's accuracy (%)	100	68	91	100	Kappa = 0.84

### 3.5. Land-Cover and Land-Use Transition Matrix in the GLHFNNR

As shown in Table 8, between 1972 and 1998, 65.74 km<sup>2</sup> (11.64%) of MDHF were turned into LDHF. In addition, between 1998 and 2007, 3.77 km<sup>2</sup> (0.67%) of Medium density MDHF were turned into LDHF. Meanwhile, between 2007 and 2013, 26.42 km<sup>2</sup> (4.68%) of MDHF were turned into LDHF.

**Table 8.** Land-cover and land-use transition matrix in the Ganjia Lake *Haloxylon* Forest National Nature Reserve from 1972 to 1998, 1998 to 2007 and 2007 to 2013 (unit: % change).

Periods		HDHF	MDHF	LDHF	Desert
1972–1998	HDHF	5.61	1.85	1.60	0.01
	MDHF	0.84	25.35	11.64	0.26
	LDHF	0.24	2.05	26.67	1.01
	Desert	0.00	0.16	0.65	22.06
1998–2007	HDHF	8.30	2.09	0.49	0.00
	MDHF	0.27	25.43	0.67	0.31
	LDHF	0.26	10.34	28.50	1.00
	Desert	0.01	0.26	0.38	21.70
2007–2013	HDHF	9.61	0.60	1.24	0.00
	MDHF	0.86	23.22	4.68	0.13
	LDHF	0.39	2.58	33.51	0.58
	Desert	0.02	0.28	0.66	21.64

Figure 8 shows the map difference in a form of stacked vertical bars. The LDHF type is predominant in all four years, comprising 40.56%, 29.98%, 40.09% and 37.06% of the total map area in 1972, 1998, 2007 and 2013, respectively (Table 6). MDHF, HDHF and desert land types were relatively stable in the total extent of each land type throughout the study period.

A slightly darker color in Figure 8 represents transition lines. To reduce visual chaos in the diagram, we used the same 0.30% threshold value in Sankey diagram to exclude unnecessary information.

The desert category remained unchanged during the study period. In the spatial extent, the net increase of the HDHF type from 1972 to 1998 and from 2007 to 2013 are attributed to conversion of MDHF (Table 8: 1.85% of map from 1972 to 1998, 2.09% from 1998 to 2007 and 0.60% from 2007 to 2013), and, to a lesser extent, the conversion of LDMF (1.60% of map from 1972 to 1998, 0.49% from 1998 to 2007 and 1.24% from 2007 to 2013).

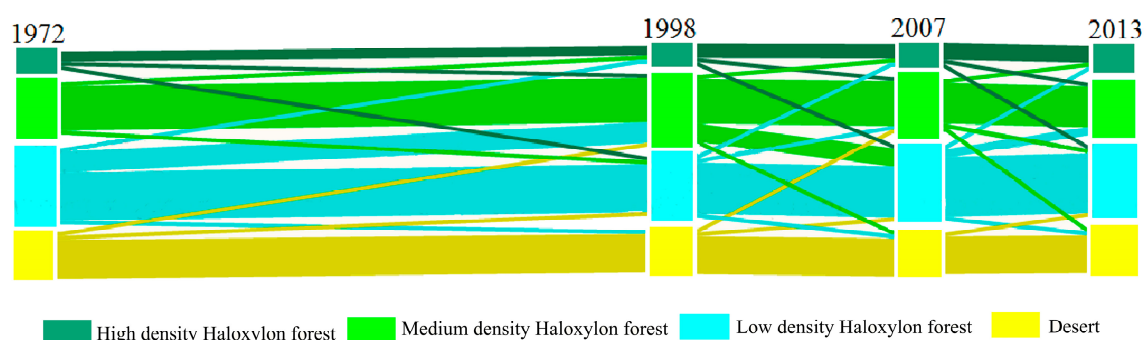


**Figure 8.** Sankey diagram of land cover dynamics from the years 1972, 1998, 2007 and 2013 in the Ganjia Lake *Haloxylon* Forest National Nature Reserve.

### 3.6. Landscape Pattern Analysis—GLHFNNR

The landscape indices of each LCLU type for the GLHFNNR were shown in Figure 9. In 1972–2013, the NP of desert are the lowest because the fragmentation degree in the surrounding of Ebinur Lake region was less (Figure 9a), and biodiversity is lesser than any other types. The LPI was compared for three different period (Figure 9b). MDHF LPI value showed a rising trend from 1972 to 2013,

suggesting that dispersed patches were merged into larger areas, decreasing the fragmentation of this LCLU type. LDHF LPI declined from 12.9725% in 1972 to 11.336% in 2013, showing that increased human activities disturbance caused dramatic fragmentation. The LSI of desert was the smallest because its shapes were more regular (Figure 9c). Different types of ecological landscapes have quite different degrees of aggregation (Figure 9d) indicating that the variety of landscapes with varying degrees of patches connection is different. CONTAG values in the GLHFNNR decreased during each period (47.43, 46.98, 45.44 and 45.30 in 1972, 1998, 2007 and 2013, respectively), indicating high levels of landscape fragmentation and declining connectivity (Figure 9e). The SHDI increased over time (1.38, 1.40, 1.40 and 1.41 in 1972, 1998, 2007 and 2013, respectively; Figure 9f), which indicated a little increase in diversity of HDHF and a trend toward monoculture land status. SHEI and IJI also had an increasing trend (Figure 9g,h), indicating that patches became more inter-conjugated and better connected into large-scale patches. The FI had a dramatic increase from 0.21 in 1972 to 0.29 in 2013 (Figure 9i).

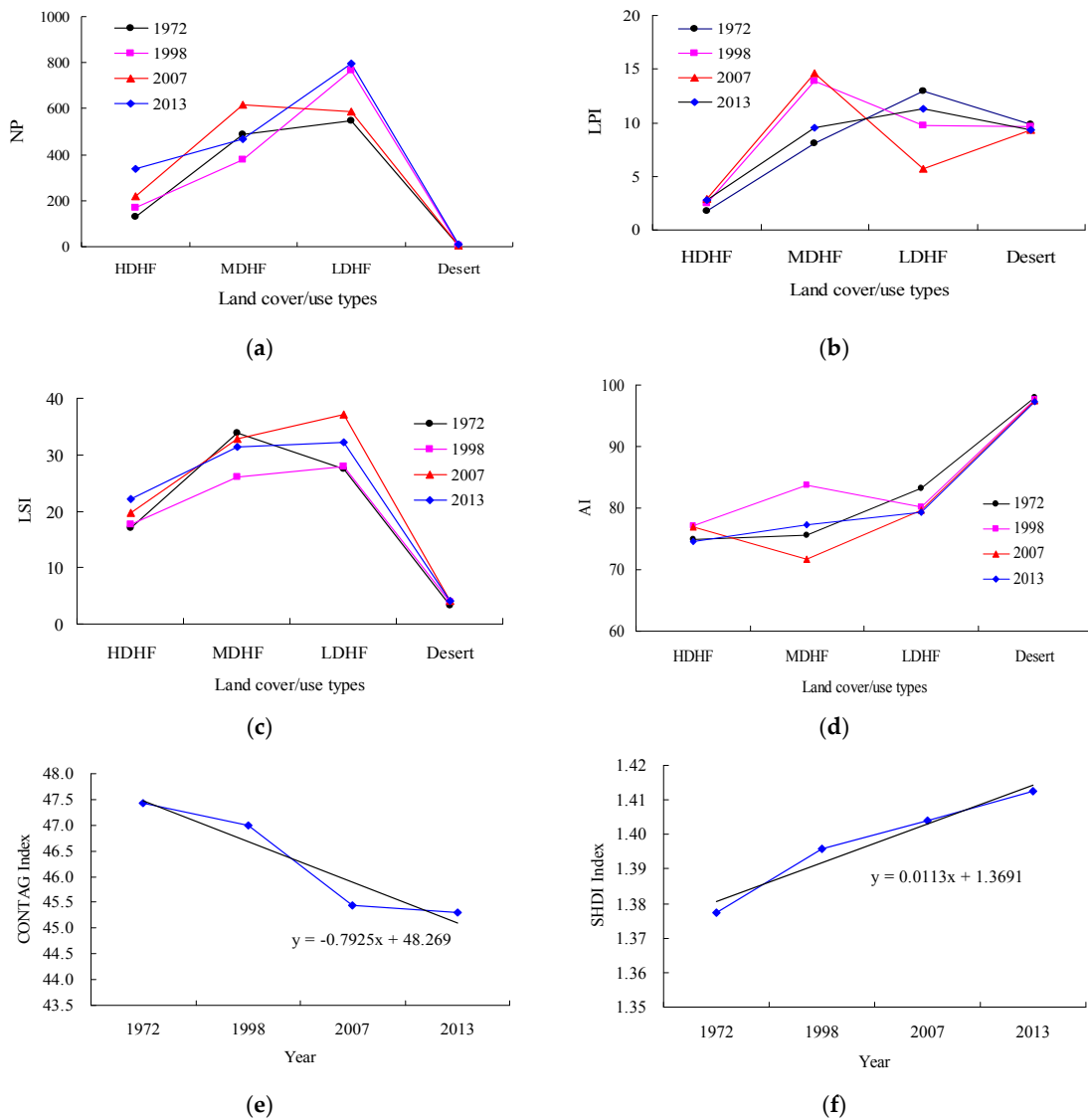
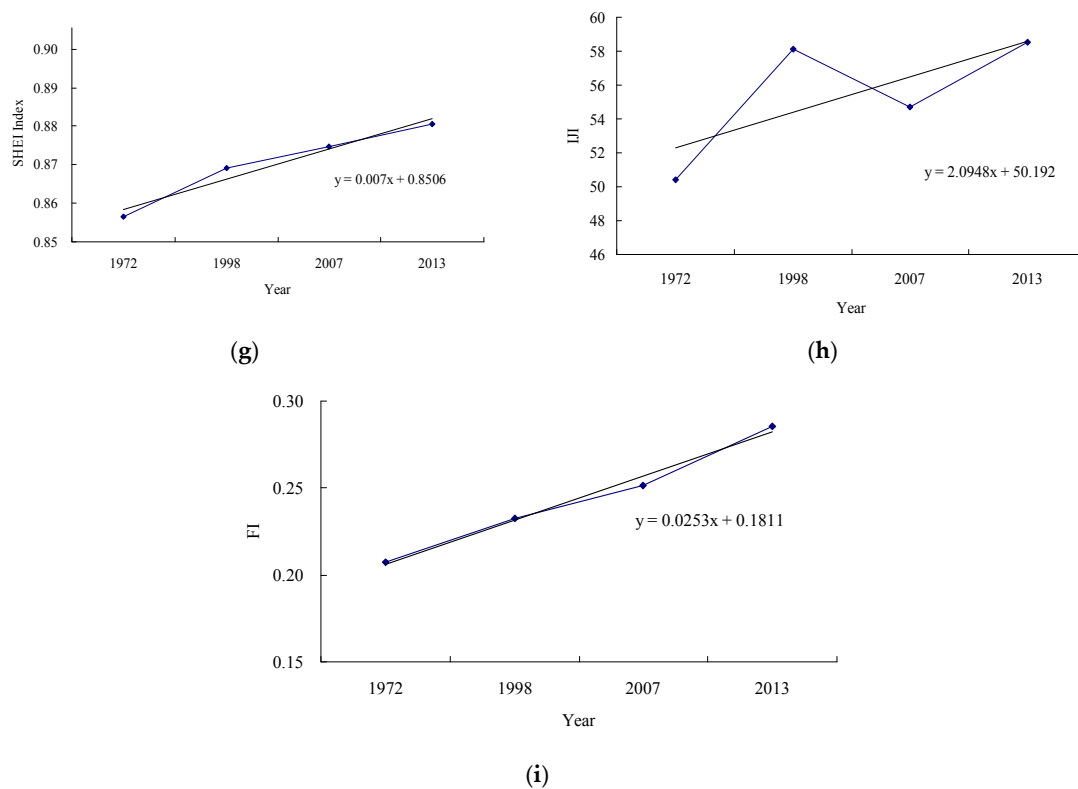


Figure 9. Cont.



**Figure 9.** Comparison of (a) NP, number of patches; (b) LPI, largest patch index; (c) LSI, landscape shape index; (d) AI, aggregation index; (e) CONTAG, contagion index; (f) SHDI, Shannon diversity index; (g) SHEI, Shannon evenness index; (h) IJI, interspersion and juxtaposition index, and (i) FI, fragmentation index, values in the Ganjia Lake *Haloxylon* Forest National Nature Reserve at five points in time: 1972 1998, 2007 and 2013. Note: LDHF, MDHF and HDHF are low, medium and high density *Haloxylon* forest, respectively.

## 4. Discussion

### 4.1. Influence of Climatic Factors on ELWNNR and GLHFNNR

Natural factors as a single force was one of the major driving forces of LCLUC processes in the region and could influence land degradation at the regional level of the landscapes [48]. “Wetland ecosystems are particularly sensitive to climate change that affects hydrology, biogeochemical processes, plant communities and ecosystem function” [49]. Precipitation and temperature determine the wet or dry local climate, affecting the formation and geographical distribution of runoff [50]. We selected annual average temperature and precipitation to study how natural factors affected the ecology of wetlands. (Figure 10). Data from the China Meteorological Data Sharing Service System (<http://cdc.nmic.cn/home.do>). Figure 10a,b show the air temperature and precipitation data, respectively.

Changes of temperature and precipitation had a significant effect on the wetland areas in the study areas. Changes in temperature leads to high evaporation in wetlands. Although there are high precipitation time to time in ELW, but the precipitation cannot supply the higher evaporation, thus rising temperatures in the ELW result in a prominent reduction in wetland and LDHF areas in the both ELWNNR and GLHFNNR region from 1959 to 2005 [19,21]. Although the annual average temperature and precipitation increased gradually from 1959 to 2005, the annual average precipitation increased slightly in a way that leads to a significant change in water resources.

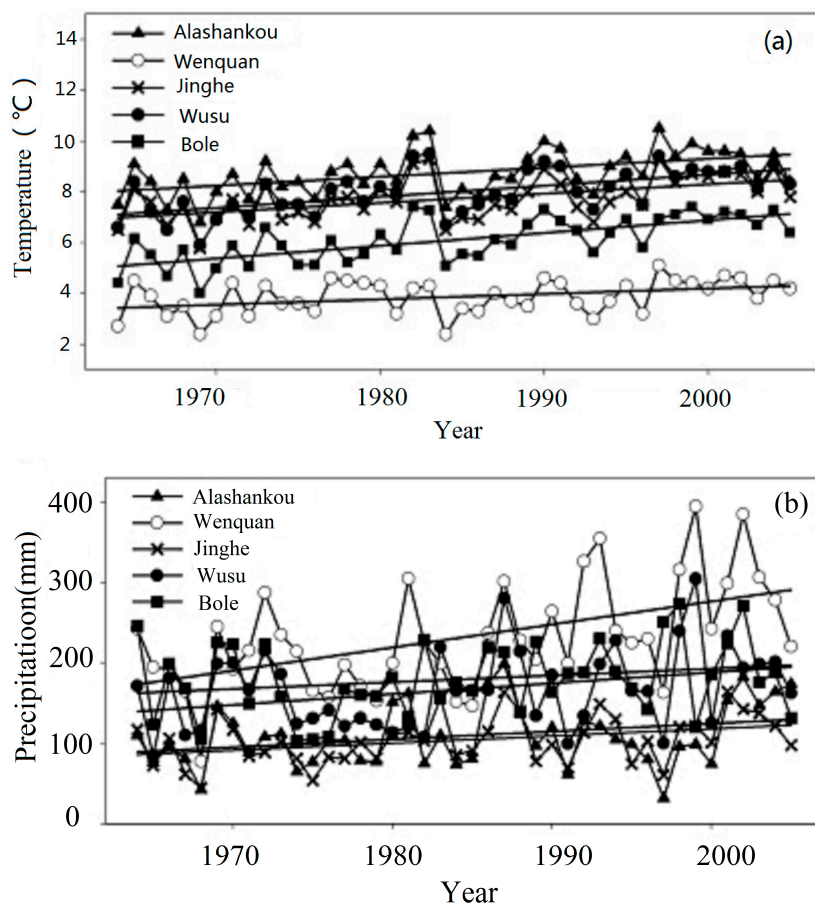


**Figure 10.** Average annual temperature (a) and precipitation (b) for 1959–2005 at the Alashankou, Bole, Jinghe, Wenquan, and Wusu meteorological stations in the study area.

#### 4.2. Influence of Human Factors on ELWNNR and GLHFNNR

Human activities appeared to be the most important factors responsible for the formation of wetland ecosystems, that is, humans are destroying many more wetlands than they are creating [51,52]. Major anthropological factors driving the changes in the study area include land use policies, population growth and agricultural water conservation. Land use policies are regulated by the national and regional government agencies. The Chinese government promote “cottons as the key to the economy”, in this area and encouraged the development of western China, including Ebinur Lake Watershed for intensive cotton farming. The Ebinur Lake Watershed produces  $7.5 \times 10^7$  kg of cotton per year [53]. The relationship between population and farmland of the Ebinur Lake Watershed from 1980 to 2007 is shown in Figure 11. Since 1950s, there have been two kinds of tillage method in Xinjiang, which are the land used by local farmer and the land intensively large scaled used by Xinjiang Production and Construction Corps for agriculture [54]. According to statistics, the population has increased from 790,000 to 1,380,000 from 1950 to 2006, and has drastically populated around ELW. The population rate went straight since 1950s and greatly enhanced the pressure on land use. Water has a critical effect on wetland ecosystems. Xinjiang Production and Construction Corps constructed dams to preserve the water for agricultural conservation in case for drought seasons. The increased use of water for irrigation on agriculture land and supporting livestock in the regions has led to a significant decline in groundwater levels (Figure 12). Meanwhile, with increase in population and farmlands in ELW, water resource exhausted and led to the succession of ecology in ELW. Forestland was preferred for land reclamation and this change led to the succession of the LCLU structure as revealed in this study. The reclamation of land by adjacent farms caused changes in the internal hydrological

conditions within the ELWNNR and GLHFNNR. Wetland areas were drastically reduced, despite their explicit protection status by the regional government. However, HDHF areas increased drastically.

This study showed that LCLUC was significant in the ELWNNR and GLHFNNR between 1972 and 2013. A large amount of wetland area has become salinized land, desert, and forestland. This study found the local water resources were insufficient to support the expansion of farm land in the Ebinur Lake Watershed; most important of all, the low water table in the surrounding region has caused droughts and habitat degradation in the ELWNNR and GLHFNNR. Therefore, our study has significant implications for the two national natural reserves that monitor and analyze the dynamics of LCLUC in the ELWNNR and GLHFNNR, explored the natural and human factors to the study area.

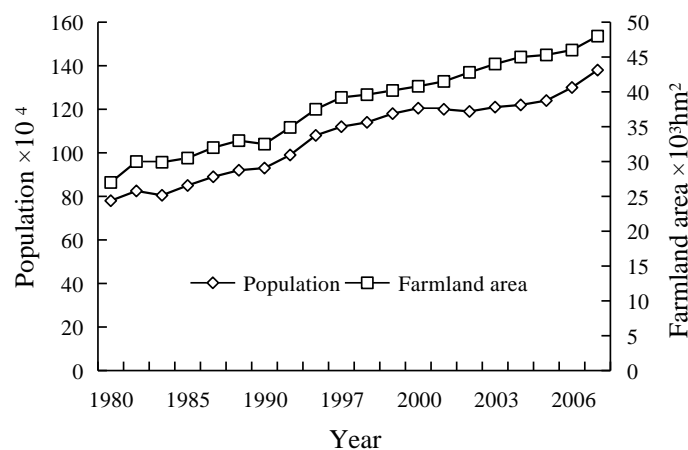


**Figure 11.** The relationship between population and farmland are within the Ebinur Lake Watershed from 1980 to 2007.

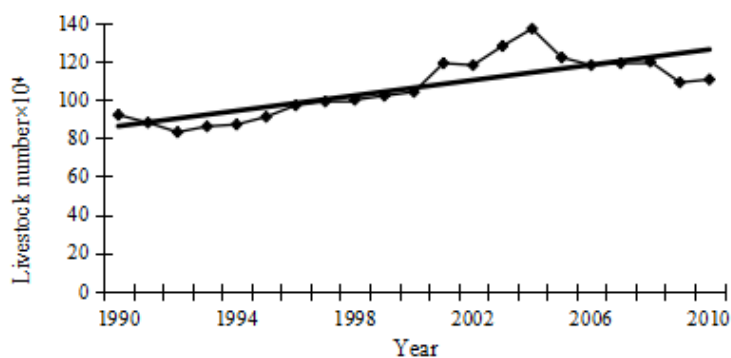


**Figure 12.** The increased stocking levels for livestock in the Ebinur Lake Watershed from 1990 to 2010.

## 5. Conclusions

Population growth and the national demand for cotton production in China have led to significant LCLUC in the ELWNNR and GLHFNNR, and surrounding Ebinur Lake Watershed between 1972 and 2013. Analysis of LCLUC showed a dramatic increase in salinized land at the expense of wetlands. Analysis of LCLUC displayed that salinized land drastically increased at the expense of wetlands. Forestland and desert areas changed less significantly, but also dramatically increased in HDHF at the expense of MDHF and LDHF. The changes in Desert area are less significant.

Landscape pattern analyses displayed a dissimilar overall pattern between the nature reserves. The NP of forestland and wetland showed that patches of these habitats were small, highly heterogeneous, scattered and fragmented. Water body and the forestland landscape shape index exhibited a growth tendency between 1972 and 2013, showed a more complex patch shape structure by contrast to other landscape types. Different types of landscapes have quite different degrees

of aggregation index, indicating that the variety of landscapes with varying degrees of patches connection is different. The Shannon evenness index is applied to describe the evenness of the patch types. The Interspersion and juxtaposition index indicated that patches became more inter-conjugated and better connected in large-scale patches, leaving only a few dominant and leading LCLU types. The Fragmentation index decreased from 0.06 in 1972 to 0.04 in 2013. The rising contagion index in the ELWNNR and Shannon diversity index values showed that growing human activities and disturbances result in the increase of wetland landscape diversity. In the nature reserve itself, wetland and forestland were similarly replaced by salinized land although in a lesser extent. Salinized land slightly replaced wetland and forestland in the nature reserve although the extent is not so much.

With the ongoing development of agriculture in Xinjiang, the location of the two reserves provides an obvious advantage. Our work demonstrated that landscape diversity in the ELWNNR and GLHFNNR are linked to the broader Ebinur Lake Watershed. To maintain a sustainable environment, making good use of ecological resources is necessary to efforts that facilitate the sustainable development of the environment on the North Slope of the economic belt of the Tianshan Mountains. Local climatic factors also have a strong effect on the formation of wetland landscapes. With the increase of temperature and precipitation since 1990s, wetland areas declined drastically. This study also highlights the prominent influence of national and local government policies on agriculture and regional water usage on wetland ecosystems in the nature reserves.

**Acknowledgments:** Thanks the National Meteorological Information Center data provided meteorological data. The research was carried out with the financial support provided by the National Natural Science Foundation of China (41361045), Xinjiang Local Outstanding Young Talent Cultivation Project of National Natural Science Foundation of China (U1503302). The authors wish to thank the referees for providing helpful suggestions to improve this manuscript.

**Author Contributions:** Fei Zhang designed the study, analyzed the data, and prepared the manuscript with contributions from Hsiang-te Kung and Verner Carl Johnson, who both also contributed data sets to this effort.

**Conflicts of Interest:** The authors declare no conflict of interest.

## References

1. Liu, H.; Weng, Q.H. Landscape metrics for analyzing urbanization-induced land use and land cover changes. *Geocarto Int.* **2013**, *28*, 582–593. [[CrossRef](#)]
2. Maimaitiyiming, M.; Ghulam, A.; Tiyp, T.; Pla, F.; Latorre-Carmona, P.; Halik, Ü.; Caetano, M. Effects of green space spatial pattern on land surface temperature: Implications for sustainable urban planning and climate change adaptation. *ISPRS J. Photogramm. Remote Sens.* **2014**, *89*, 59–66. [[CrossRef](#)]
3. Jackson, S.T.; Sax, D.F. Balancing biodiversity in a changing environment: Extinction debt, immigration credit and species turnover. *Trends Ecol. Evolut.* **2010**, *25*, 153–160. [[CrossRef](#)] [[PubMed](#)]
4. Baan, L.; Alkemade, R.; Koellner, T. Land use impacts on biodiversity in LCA: A global approach. *Int. J. Life Cycle Assess.* **2012**, *18*, 1216–1230. [[CrossRef](#)]
5. Dirzo, R.; Raven, P.H. Global state of biodiversity and loss. *Ann. Rev. Environ. Resour.* **2003**, *28*, 137–167. [[CrossRef](#)]
6. Didham, R.K.; Kapos, V.; Ewers, R.M. Rethinking the conceptual foundations of habitat fragmentation research. *Oikos* **2012**, *121*, 161–170. [[CrossRef](#)]
7. Ghulam, A. Monitoring Tropical Forest Degradation in Betampona Nature Reserve, Madagascar Using Multisource Remote Sensing Data Fusion. *IEEE J. Sel. Top. Appl. Earth Obs. Remote Sens.* **2014**, *7*, 4960–4971. [[CrossRef](#)]
8. Ghulam, A.; Ghulam, O.; Maimaitijiang, M.; Freeman, K.; Porton, I.; Maimaitiyiming, M. Remote Sensing Based Spatial Statistics to Document Tropical Rainforest Transition Pathways. *Remote Sens.* **2015**, *7*, 6257–6279. [[CrossRef](#)]
9. Reid, R.S.; Kruska, R.L.; Muthui, N.; Taye, A.; Wotton, S.; Wilson, C.J.; Mulatu, W. Land-use and land-cover dynamics in response to changes in climatic, biological and socio-political forces: The case of southwestern Ethiopia. *Landsc. Ecol.* **2000**, *15*, 339–355. [[CrossRef](#)]
10. Jin, G.; Wang, P.; Zhao, T.; Bai, Y.P.; Zhao, C.H.; Dong, C. Reviews on land use change induced effects on regional hydrological ecosystem services for integrated water resources management. *Phys. Chem. Earth Parts A/B/C* **2015**, *89*, 33–39. [[CrossRef](#)]

11. Meshesha, T.W.; Tripathi, S.K.; Khare, D. Analyses of land use and land cover change dynamics using GIS and remote sensing during 1984 and 2015 in the Beressa Watershed Northern Central Highland of Ethiopia. *Model. Earth Syst. Environ.* **2016**, *2*, 168–180. [[CrossRef](#)]
12. Liu, G.L.; Zhang, L.C.; Zhang, Q.; Musyimi, Z.; Jiang, Q.H. Spatio-temporal dynamics of wetland landscape patterns based on Remote Sensing in Yellow River Delta, China. *Wetlands* **2014**, *34*, 787–801. [[CrossRef](#)]
13. FRAGSTATS v3: Spatial Pattern Analysis Program for Categorical Maps. Computer Software Program Produced by the Authors at the University of Massachusetts, Amherst. Available online: <http://www.umass.edu/landeco/research/fragstats/fragstats.html> (accessed on 30 April 2017).
14. Copeland, H.E.; Tessman, S.A.; Girvetz, E.H.; Roberts, L.; Enquist, C.; Orabona, A.; Patla, S.; Kiesecker, J. A geospatial assessment on the distribution, condition, and vulnerability of Wyoming's wetlands. *Ecol. Indic.* **2010**, *10*, 869–879. [[CrossRef](#)]
15. Sulman, B.; Desai, A.; Mladenoff, D. Modeling soil and biomass carbon responses to declining water table in a wetland-rich landscape. *Ecosystems* **2013**, *16*, 491–507. [[CrossRef](#)]
16. Robertson, L.D.; King, D.J.; Davies, C. Assessing Land Cover Change and Anthropogenic Disturbance in Wetlands Using Vegetation Fractions Derived from Landsat 5 TM Imagery (1984–2010). *Wetlands* **2015**, *35*, 1077–1091. [[CrossRef](#)]
17. Zhang, H.; Qi, Z.F.; Ye, X.Y.; Cai, Y.B.; Ma, W.C.; Chen, M.N. Analysis of land use/land cover change, population shift, and their effects on spatiotemporal patterns of urban heat islands in metropolitan Shanghai, China. *Appl. Geogr.* **2013**, *44*, 121–133. [[CrossRef](#)]
18. Yao, J.Q.; Liu, Z.H.; Yang, Q.; Meng, X.Y.; Li, C.Z. Responses of Runoff to Climate Change and Human Activities in the Ebinur Lake Catchment, Western China. *Water Resour.* **2014**, *41*, 738–747. [[CrossRef](#)]
19. Wang, L.; Ding, J.L. Vegetation index feature change and its influencing factors and spatial-temporal process analysis of desert grassland in the Ebinur Lake Nature Reserve, Xinjiang. *Acta Prataculturae Sin.* **2015**, *24*, 4–11. [[CrossRef](#)]
20. Ma, Q. Land use dynamic change and associated effects on eco-environment in Gan-jia lake wetland. *J. Arid Land Resour. Environ.* **2012**, *26*, 189–194.
21. Zhang, F.; Tashpolat, T.; Verner, C.J.; Kung, H.T.; Ding, J.L.; Sun, Q.; Zhou, M.; Ardak, K.; Ilyas, N.; Chan, N.W. The influence of natural and human factors in the shrinking of the Ebinur Lake, Xinjiang, China, during the 1972–2013 period. *Environ. Monit. Assess.* **2015**, *187*, 4128–4142. [[CrossRef](#)] [[PubMed](#)]
22. Wang, Y.; Li, Y.; Xiao, D. Catchment scale spatial variability of soil salt content in agricultural oasis, Northwest China. *Environ. Geol.* **2008**, *56*, 439–446. [[CrossRef](#)]
23. Metternicht, G.; Zinck, J.A. *Remote Sensing of Soil Salinization: Impact on Land Management*; CRC Press: Boca Raton, FL, USA, 2008.
24. Jia, K.; Liang, S.L.; Zhang, N.; Wei, X.Q.; Gu, X.F.; Zhao, X.; Yao, Y.J.; Xie, X.H. Land cover classification of finer resolution remote sensing data integrating temporal features from time series coarser resolution data. *ISPRS J. Photogramm. Remote Sens.* **2014**, *93*, 49–55. [[CrossRef](#)]
25. Friedl, M.A.; Brodley, C.E. Decision tree classification of land cover from remotely sensed data. *Remote Sens. Environ.* **1997**, *61*, 399–409. [[CrossRef](#)]
26. Pal, M.; Mather, P.M. An assessment of the effectiveness of decision tree methods for land cover classification. *Remote Sens. Environ.* **2003**, *86*, 554–565. [[CrossRef](#)]
27. Keuchel, J.; Naumann, S.; Heiler, M. Automatic land cover analysis for Tenerife by supervised classification using remotely sensed data. *Remote Sens. Environ.* **2003**, *86*, 530–541. [[CrossRef](#)]
28. Zhang, F.; Tashpolat, T.; Feng, Z.D.; Kung, H.T.; Verner, C.J.; Ding, J.L.; Nigela, T.; Maimaiti, S.; Gui, D.W. Spatio-temporal patterns of land use/cover changes over the past 20 years in the middle reaches of the Tarim River, Xinjiang, China. *Land Degrad. Dev.* **2015**, *26*, 284–299. [[CrossRef](#)]
29. Richards, J.A.; Jia, X. *Remote Sensing Digital Image Analysis, an Introduction*, 4th ed.; Springer: Berlin, Germany, 2006.
30. Pradhan, B.; Sulaiman, Z. Land cover mapping and spectral analysis using multi-sensor satellite data: A case study in Tioman Island, Malaysia. *J. Geomat.* **2009**, *3*, 71–78.
31. Biro, K.; Pradhan, B.; Buchroithner, M.; Makeschin, F. Land use/land cover change analysis and its impact on soil properties in the Northern part of Gadarif region, Sudan. *Land Degrad. Dev.* **2013**, *24*, 90–102. [[CrossRef](#)]
32. Sun, J.B.; Yang, J.Y.; Zhang, C.; Yun, W.J.; Qu, J.Q. Automatic remotely sensed image classification in a grid environment based on the maximum likelihood method. *Math. Comput. Model.* **2013**, *58*, 573–581. [[CrossRef](#)]

33. Banerjee, R.; Srivastava, P.K. Reconstruction of contested landscape: Detecting land cover transformation hosting cultural heritage sites from Central India using remote sensing. *Land Use Policy* **2013**, *34*, 193–203. [CrossRef]
34. Shao, Y.; Lunetta, R.S.; Wheeler, B.; Iiames, J.S.; Campbell, J.B. An evaluation of time-series smoothing algorithms for land-cover classifications using MODIS-NDVI multitemporal data. *Remote Sens. Environ.* **2016**, *174*, 258–265. [CrossRef]
35. Smeeton, N.C. Early History of the Kappa Statistic. *Biometrics* **1985**, *41*, 795.
36. Fleiss, J.L. *Statistical Methods for Rates and Proportions*, 2nd ed.; John Wiley: New York, NY, USA, 1981.
37. Wan, L.H.; Zhang, Y.W.; Zhang, X.Y.; Qi, S.Q.; Na, X.D. Comparison of land use/land cover change and landscape patterns in Honghe National Nature Reserve and the surrounding Jiانشanjiang Region, China. *Ecol. Indic.* **2015**, *51*, 205–214. [CrossRef]
38. Schmidt, M. The Sankey diagram in energy and material flow management, part I: History. *J. Ind. Ecol.* **2008**, *12*, 82–94. [CrossRef]
39. Cuba, N. Research note: Sankey diagrams for visualizing land cover dynamics. *Landsc. Urban Plan.* **2015**, *139*, 163–167. [CrossRef]
40. Paukert, C.P.; Pitts, K.L.; Whittier, J.B.; Olden, J.D. Development and assessment of a landscape-scale ecological threat index for the Lower Colorado River Basin. *Ecol. Indic.* **2011**, *11*, 304–310. [CrossRef]
41. Seto, K.C.; Fragkias, M. Quantifying spatial-temporal patterns of urban land-use change in four cities of China with time series landscape metrics. *Landsc. Ecol.* **2005**, *20*, 871–888. [CrossRef]
42. Xu, K.; Kong, C.F.; Liu, G.; Wu, C.L.; Deng, H.B.; Zhang, Y. Changes of urban wetlands in Wuhan, China, from 1987 to 2005. *Prog. Phys. Geogr.* **2010**, *34*, 207–220.
43. EPA (Environmental Protection Agency). A Landscape Approach for Detecting and Evaluating Change in a Semi-Arid Environment, Office of Research and Development, Washington, DC, USA. EPA 620/R-94/009; 2000. Available online: <http://www.epa.gov/crdlvweb/land-sci/san-pedro.htm> (accessed on 19 January 2017).
44. Fan, Q.D.; Ding, S.Y. Landscape pattern changes at a county scale: A case study in Fengqiu, Henan Province, China from 1990 to 2013. *CATENA* **2016**, *137*, 152–160. [CrossRef]
45. Wang, S.; Ding, J.L.; Wang, L.; Niu, Z.Y. Response of ecological service value to land use change in nearly 20 years in Ebinur Lake region of Xinjiang based on remote sensing. *Res. Soil Water Conserv.* **2014**, *21*, 144–149.
46. Ma, L.; Wu, J.L.; Liu, W.; Abuduwaili, J.L.L. Distinguishing between anthropogenic and climatic impacts on lake size: A modeling approach using data from Ebinur Lake in arid northwest China. *J. Limnol.* **2014**, *73*, 350–357. [CrossRef]
47. Qiang, A.G.; Li, Q.C. Anthropogenic interference analysis of Ganjia Lake Haloxylon forest National Nature Reserve in Xinjiang. *Jilin Agric.* **2013**, *3*, 206–207.
48. Dawelbait, M.; Morari, F. Monitoring desertification in a Savannah region in Sudan using Landsat images and spectral mixture analysis. *J. Arid Environ.* **2012**, *80*, 45–55. [CrossRef]
49. Malekmohammadi, B.; Blouchi, L.R. Ecological risk assessment of wetland ecosystems using multi criteria decision making and geographic information system. *Ecol. Indic.* **2014**, *41*, 133–144. [CrossRef]
50. Shi, Y.F.; Shen, Y.P.; Li, D.L.; Zhang, G.W.; Ding, Y.J.; Hu, R.J.; Kang, E. Discussion on the present climate change from WARM-DRY to WARM-WET in northwest CHINA. *Quat. Sci.* **2003**, *23*, 152–164.
51. Zhang, F.; Tashpolat, T.; Verner, C.J.; Kung, H.T.; Ding, J.L.; Zhou, M.; Fan, Y.H.; Ardak, K.; Ilyas, N. Evaluation of land desertification from 1990 to 2010 and its causes in Ebinur Lake region, Xinjiang China. *Environ. Earth Sci.* **2015**, *73*, 5731–5745. [CrossRef]
52. Wang, T.; Yan, C.Z.; Song, X.; Xie, J.L. Monitoring recent trends in the area of aeolian desertified land using Landsat images in China's Xinjiang region. *ISPRS J. Photogramm. Remote Sens.* **2012**, *68*, 184–190. [CrossRef]
53. Ge, L.M. Study on Climatic Variation and Its Effect in Recent 45 Years in Ebinur Lake Basin of Xinjiang. Master's Thesis, Xinjiang University, Ürümqi, China, 2006.
54. Wang, S.X.; Wang, S.L. Land use/land cover change and their effects on landscape patterns in the Yanqi Basin, Xinjiang (China). *Environ. Monit. Assess.* **2013**, *185*, 9729–9742. [CrossRef] [PubMed]

